



# A 9000-year carbon isotopic record of acid-soluble organic matter in a stalagmite from Heshang Cave, central China: Paleoclimate implications



Xiuli Li<sup>a</sup>, Chaoyong Hu<sup>a,\*</sup>, Junhua Huang<sup>b</sup>, Shucheng Xie<sup>a</sup>, Andy Baker<sup>c</sup>

<sup>a</sup> State Key Laboratory of Biogeology and Environmental Geology, China University of Geosciences, Wuhan, Hubei 430074, China

<sup>b</sup> State Key Laboratory of Geological Processes and Mineral Resources, China University of Geosciences, Wuhan 430074, China

<sup>c</sup> Connected Waters Initiative Research Centre, UNSW Australia, NSW 2052, Australia

## ARTICLE INFO

### Article history:

Received 7 November 2013

Received in revised form 8 July 2014

Accepted 31 August 2014

Available online 16 September 2014

Editor: Michael E. Böttcher

### Keywords:

Acid-soluble organic matter

Stalagmite

Organic carbon isotope

Soil ecosystem

Microbial activity

## ABSTRACT

Organic matter preserved in speleothems has the potential to reflect the changes of the overlying vegetation and soil ecosystem. Here we report the first near 50-yr-resolution acid-soluble organic matter (ASOM) carbon isotope ( $\delta^{13}\text{C}_{\text{ASOM}}$ ) sequence derived from a laminated stalagmite (HS-4) spanning the last 9 ky in Heshang Cave, central China. The  $\delta^{13}\text{C}_{\text{ASOM}}$  values vary between  $-25.8\%$  and  $-22.0\%$ , with lower values from 9 to 4 ka BP and less negative values from 4 to 0 ka BP. We postulate that the  $\delta^{13}\text{C}_{\text{ASOM}}$  sequence is mainly controlled by temperature and water balance. Temperature could affect both vegetation physiology and microbial degradation in soil horizons. The influence of temperature on the  $\delta^{13}\text{C}_{\text{ASOM}}$  is supported by the negative correlation ( $r = -0.48$ ,  $p < 0.001$ ) between the  $\delta^{13}\text{C}_{\text{ASOM}}$  record and the paleotemperature record in the nearby Dajiuhu peatland. The water balance can affect the retention time of organic matter in soils. Under drier conditions, the soil organic matter will be retained longer and is more likely to be biologically degraded, resulting in more negative  $\delta^{13}\text{C}_{\text{ASOM}}$  values. Our results reveal that  $\delta^{13}\text{C}_{\text{ASOM}}$  in speleothems has the potential to reflect the response of vegetation and/or soil processes to paleoclimate changes.

© 2014 Elsevier B.V. All rights reserved.

## 1. Introduction

Stalagmites are one of the most important archives for high-resolution paleoclimate reconstructions in the Quaternary, with many climatic proxies developed (McDermott, 2004; Blyth et al., 2008; Fairchild and Treble, 2009). Among these proxies, the carbon isotope composition of calcite ( $\delta^{13}\text{C}_{\text{carb}}$ ) has been widely investigated and is normally interpreted as an indicator of overlying vegetation changes (e.g. Genty et al., 2001; Frappier et al., 2002; McDermott, 2004; Cosford et al., 2009). However, the carbon isotopic signal of dissolved  $\text{CO}_2$  can be affected by other processes, especially fractionation during carbonate precipitation and degassing (Baker et al., 2011; Dreybrodt and Scholz, 2011; Frisia et al., 2011), leaving an uncertainty in the interpretation of  $\delta^{13}\text{C}_{\text{carb}}$  as a record of vegetation (e.g. Genty et al., 2003; Blyth et al., 2007).

In comparison to inorganic carbon, organic matter acts as a minor carbon pool in speleothems. Plenty of researchers have exploited the paleoecological and paleoenvironmental potential of lipid biomarkers in speleothems (e.g. Xie et al., 2003; Blyth et al., 2008, 2014; Huang et al., 2008a, 2008b; Rushdi et al., 2011; Yang et al., 2011; Blyth and Schouten, 2013). Other than lipid biomarkers, humic substances, especially fulvic acids have been widely investigated due to their

luminescence features, which correlate with the overlying soil and vegetation changes (McGarry and Baker, 2000; Fairchild and Baker, 2012). Both fluorescence analysis and TOC monitoring of drip water reveal that fulvic acids are the predominant humic substances in drip water and speleothems (van Beynen et al., 2002; Smailer and White, 2013).

The  $\delta^{13}\text{C}$  values of organic matter ( $\delta^{13}\text{C}_{\text{org}}$ ) in speleothems have considerable importance in paleoenvironmental research (Blyth et al., 2013a, 2013b), as they have the potential to directly record how the overlying soil ecosystem responses to paleoclimate changes. Studies using  $\delta^{13}\text{C}_{\text{org}}$  in karst systems are quite limited. A few studies have discussed  $\delta^{13}\text{C}_{\text{org}}$  in cave sediments (Turney et al., 2001; Panno et al., 2004; Polk et al., 2007, 2013). Polk et al. (2013) used carbon isotopes from fulvic acids (FAs) in cave sediments to develop a record of vegetation over the last 3000 yr. Recently Blyth et al. (2013a) developed a novel liquid chromatography–isotope ratio mass spectrometry to determine the  $\delta^{13}\text{C}$  values of non-purgeable organic carbon (NPOC) in speleothems. Immediately, Blyth et al. (2013b) reported a time series of the  $\delta^{13}\text{C}$  of NPOC and long chain *n*-alkanes from a 2000-year old Scotland stalagmite, and demonstrated a negative correlation between NPOC and carbonate isotope values. They hypothesized that this was due to preferential use of  $^{12}\text{C}$  by microbes during periods of increased activity, resulting in enrichment of the residual OM, and depletion of the  $\text{CO}_2$ . The above studies highlight that the  $\delta^{13}\text{C}$  of the organic matter pool in cave systems has the potential to track the paleoenvironmental changes.

\* Corresponding author.

E-mail address: [chyhu@cug.edu.cn](mailto:chyhu@cug.edu.cn) (C. Hu).

In this study, we isolated acid-soluble organic matter (ASOM) from an absolutely dated stalagmite (HS-4) from Heshang Cave and measured the carbon isotope composition using a relatively small amount of rock sample (ca. 2 g). We conducted infrared spectroscopy (IR) analysis to provide evidence that the extracted ASOM mainly originates from the overlying soil organic matter. Then we discuss the plausible processes affecting the ASOM carbon isotope ( $\delta^{13}\text{C}_{\text{ASOM}}$ ) variations in HS-4 stalagmite over the last 9 ky.

## 2. Materials and methods

### 2.1. Locality and sampling

Heshang Cave (30°27'N, 110°25'E, 294 m altitude) is located on the south bank of the Qingjiang River, a large tributary of the Yangtze River in central China (Fig. 1). The geographic and climatic settings of this cave have been shown in detail in Hu et al. (2008a). In general, this region is affected mostly by the East Asian monsoon, with high temperatures and high precipitation in summer months.

The samples used in this study were collected from the HS-4 stalagmite (Hu et al., 2008b). This stalagmite (2.54 m in length) was still actively growing when it was removed. The chronology of HS-4 was established independently by U–Th dating and layer counting (Hu et al., 2008b). In order to avoid organic contamination, all stalagmite samples were selected from the fresh internal parts after discarding the surface layer (Hu et al., 2008b). In total, using a dental-drill, 170 samples were collected from HS-4, all of 1–2 cm thickness and parallel to the growth layers. HS-4 stalagmite has an approximately constant growth rate, averaging 0.27 mm per year (Hu et al., 2008b). Thus the temporal resolution of the samples for ASOM analysis is about 40–80 years. At one location (173 cm from the top), four samples were collected within a single growth layer.

Surface samples were collected from the overlying soil (0–2 cm; 30°2.334'N, 110°25.148'E, 961 m altitude) above Heshang Cave in July and November 2012. A subsoil sample was collected from the soil profile (97–103 cm depth below surface; November 2012). In addition,

two drip water samples (ca. 4 L in a brown bottle) were collected at the former growth site of HS-4 stalagmite in July and November 2012. In addition, a limestone sample was collected from the bedrock of Heshang Cave.

### 2.2. ASOM extraction

The stalagmite samples were air-dried and crushed to pass an 80-mesh sieve. The powdered stalagmite samples (ca. 2 g) were dissolved in 6 M HCl and kept overnight. Then the acid solution (pH < 2) was centrifuged at a rate of 8000 r/s to separate the supernatant and insoluble matter. The supernatant was freeze-dried and is referred as ASOM in this study. After acid dissolution, the insoluble fraction was near absent. Thus we only focused on the acid soluble fraction in this study. The soil samples were air-dried at room temperature and then were treated by the same procedure as the stalagmites. Water samples (ca. 0.5 L) were evaporated to dryness at 60 °C and were subsequently treated in the same manner as the soil and stalagmite samples.

Three stalagmite samples (33.0 cm, 118.4 cm, 198.4 cm to the top) were selected for analysis of ASOM concentration using TOC/TC analyzer (Analytik Jena AG Multi N C 3100). The reproducibility was less than 1.5%.

### 2.3. Carbon isotope composition analysis

The carbon isotopic compositions of the ASOM were determined via continuous flow on a Thermo Flash Elemental Analyzer (EA) coupled with a Thermo MAT-253 isotope ratio mass spectrometer (IRMS) at Nanjing Center, Geological Survey Bureau of China (NJ) and State Key Laboratory of Geological Processes and Mineral Resources, China University of Geosciences at Wuhan (WH). The ASOM was oxidized to CO<sub>2</sub> at 1000 °C with chromium oxide. The carbon isotope composition in the resultant CO<sub>2</sub> was measured by a MAT-253 mass spectrometer. The  $\delta^{13}\text{C}_{\text{ASOM}}$  values were normalized to the VPDB (Vienna Pee Dee Belemnite) standard using a charcoal reference material (GBW04407, with a  $\delta^{13}\text{C}$  value of  $-22.43\text{‰}$ ). The long-term reproducibility of the

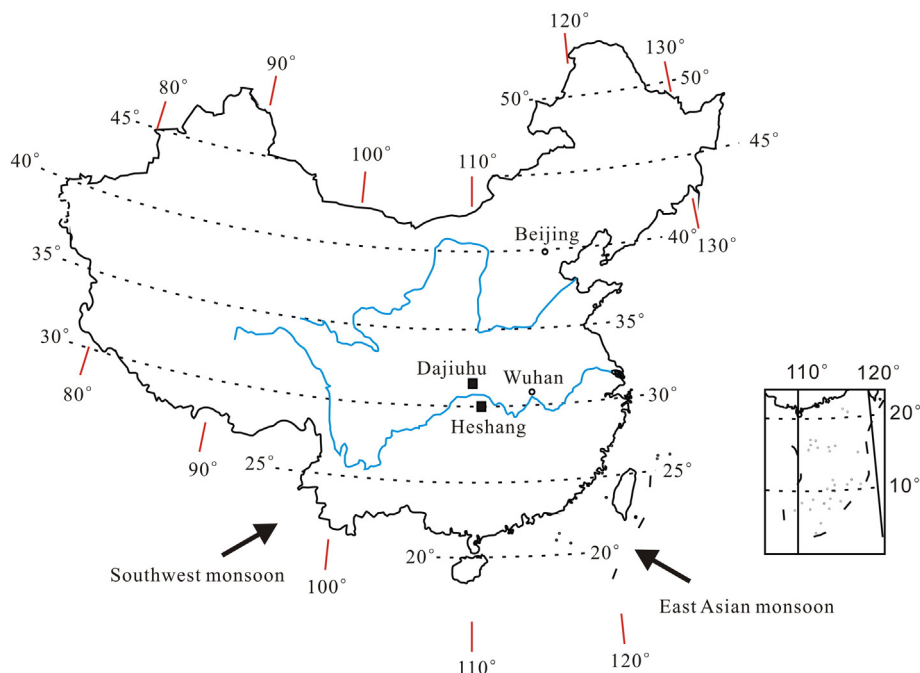


Fig. 1. Locality of Heshang Cave in China.

internal standards was better than 0.2%. It is cautioned that the precipitated acid salts can to some extent affect the EA performance.

## 2.4. Spectroscopic analyses

### 2.4.1. IR analyses

IR analyses on selected soil, drip water, bedrock and stalagmite samples were performed on a Thermo Fisher Nicolet 6700 Fourier transform infrared spectrometer (FT-IR) at the School of Material and Chemistry, China University of Geosciences, Wuhan. The freeze-dried ASOM was crushed in a mortar and mixed with potassium bromide (KBr, FT-IR grade) at a ratio of 1:200 and pressed into pellets. These pellets were investigated in transmission mode in the mid-infrared range ( $4000\text{--}400\text{ cm}^{-1}$ ) with 32 scans per spectrum and a resolution of  $4\text{ cm}^{-1}$ . The spectra were evaluated after height normalization and automatic baseline correction by using the evaluation software provided with the FT-IR spectrometer.

### 2.4.2. Synchronous fluorescence analysis

Recently, we reported an improved synchronous fluorimetric method for the determination of dissolved organic matter in cave drip water (Li et al., *in press*). Briefly, the stalagmite samples were dissolved in dilute HCl. Then an aliquot (ca. 10 mL) was transferred to a 25 mL test tube and ascorbic acid was added. Fluorescence analysis was conducted with a PerkinElmer LS-55 Luminescence Spectrophotometer using a 150 W Xe lamp. The synchronous fluorescence intensity (SFI) was measured using a 1 cm quartz cell with wavelength scanning from 200 nm to 500 nm with  $\Delta\lambda$  at 20 nm.

## 3. Results

### 3.1. ASOM spectroscopic results

The ASOM extracts from the overlying soil, drip water and stalagmite show similar IR spectra, exhibiting a strong and wide absorption band near  $3400\text{ cm}^{-1}$  and a secondary band at  $1630\text{ cm}^{-1}$  (Fig. 2).

The former corresponds with the stretching vibrational absorption of phenolic O–H bond, whereas the latter relates with the stacked absorption peaks of C=C and C=O groups and associated hydrogen bonds (Kim et al., 1990). These spectra are quite typical of those reported for fulvic-acids (Stevenson and Goh, 1971; Senesi et al., 1989; Kim et al., 1990). Comparing the bedrock sample to the soil, water and stalagmite samples, the bedrock shows a quite different IR spectrum, with strong absorption bands near  $3667$ ,  $3069$ ,  $2258$  and  $1677$ , and  $1601\text{ cm}^{-1}$  (Fig. 2), which is similar to the spectra of matured kerogen (Lis et al., 2005). During the synchronous fluorescence analysis, the wavelength of maximum fluorescence intensity of the HS-4 stalagmite samples varies between 391 nm and 385 nm and displays a general decreasing trend with time (Fig. 3). The interval between 1.6 and 0 ka has relatively low wavelength of maximum fluorescence.

### 3.2. Carbon isotopic composition of ASOM

Three samples have been analyzed to determine the concentration of ASOM. These three samples show low but constant ASOM content ( $0.12\text{--}0.14\text{ mg/g calcite}$ ). The ASOM concentration is similar with the TOC concentration in Blyth et al. (2013a;  $0.11\text{ mg/g calcite}$ ), but lower than the TOC concentration in BW-1 stalagmite from Beijing, China (Duan et al., 2014;  $0.6\text{--}2.5\text{ mg/g calcite}$ ).

The isotopic compositions of our samples were analyzed on two different EA-IRMS systems. In order to check for any inter-laboratory differences, three samples (HS4-13, HS4-56 and HS4-133) were selected to be analyzed at both laboratories. These samples exhibit quite similar  $\delta^{13}\text{C}_{\text{ASOM}}$  values, with deviation less than 0.1‰. The reproducibility of our ASOM extraction procedure was evaluated by triplicate treatment of selected samples (HS4-56 and HS4-132) using the same procedure. These results show relatively small derivations (0.1‰ and 0.4‰, respectively). Thus we assume the analytical error for  $\delta^{13}\text{C}_{\text{ASOM}}$  in this study is between 0.2 and 0.4‰, which is relatively higher than the long-term repeatability of  $\delta^{13}\text{C}_{\text{carb}}$  (0.1‰; Hu et al., 2008b).

Four sub-samples (HS4-C1–HS4-C4) were collected across the single growth layer (173 cm from the top) for  $\delta^{13}\text{C}_{\text{carb}}$  and  $\delta^{13}\text{C}_{\text{ASOM}}$

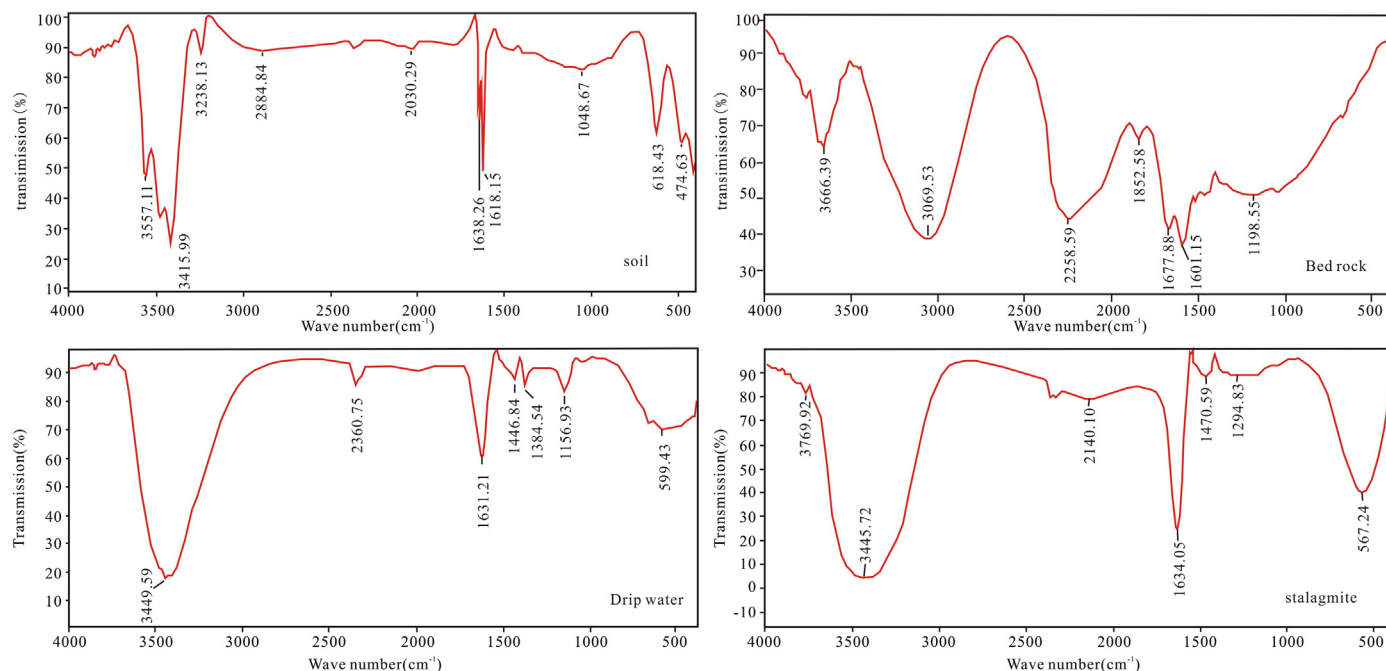
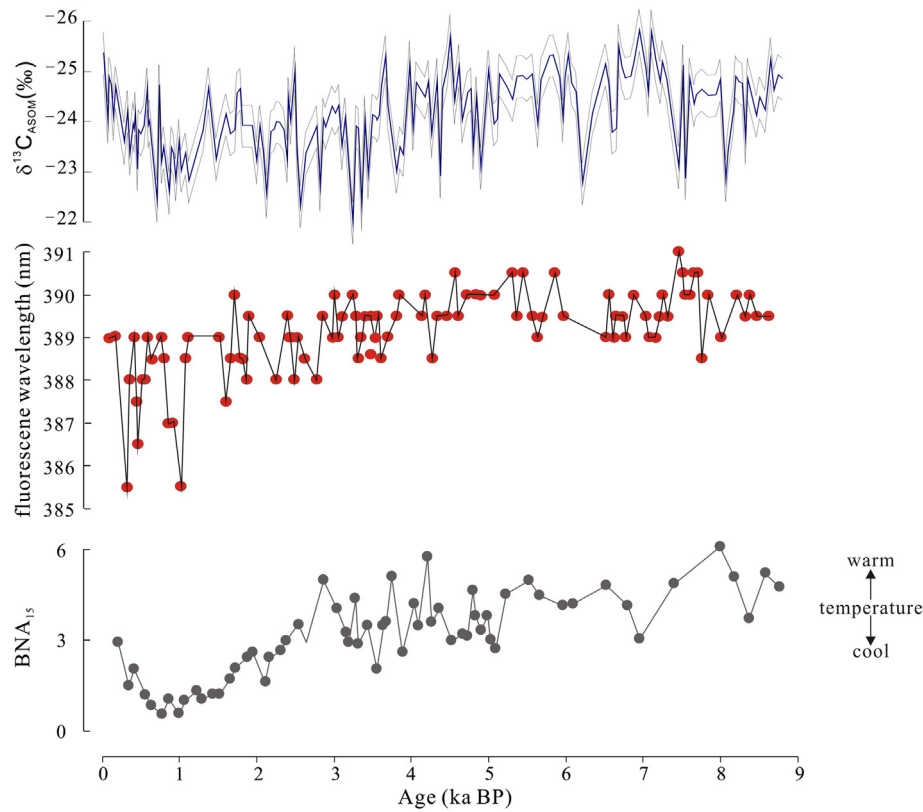


Fig. 2. FT-IR spectra of ASOM isolated from the overlying soil, bedrock, drip water and stalagmite samples.



**Fig. 3.** Comparison of  $\delta^{13}\text{C}_{\text{ASOM}}$ , and the synchronous fluorescence wavelength in HS-4 stalagmite and paleotemperature reconstructed in the Dajiuhe peatland (Huang et al., 2013) over the last 9 ky. The dashed lines above and below the  $\delta^{13}\text{C}_{\text{ASOM}}$  curve refer to the analytical error of 0.4‰.

analyses. The  $\delta^{13}\text{C}_{\text{carb}}$  values progressively become larger towards the edge, with a variation of ca. 2‰ (Hu et al., 2008b; Fig. 4). In contrast,  $\delta^{13}\text{C}_{\text{ASOM}}$  shows quite small variation (<0.3‰) in the single growth layer (Fig. 4).

The  $\delta^{13}\text{C}_{\text{ASOM}}$  values of HS-4 range from  $-25.8$  to  $-22.0$ ‰, averaging  $-24.2$ ‰ (Fig. 3). The  $\delta^{13}\text{C}_{\text{ASOM}}$  values are relatively more negative during the period from 9 to 4 ky BP (averaging  $-24.6$ ‰) and less negative from 4 to 0 ky BP (averaging  $-23.8$ ‰). In contrast, the  $\delta^{13}\text{C}_{\text{carb}}$

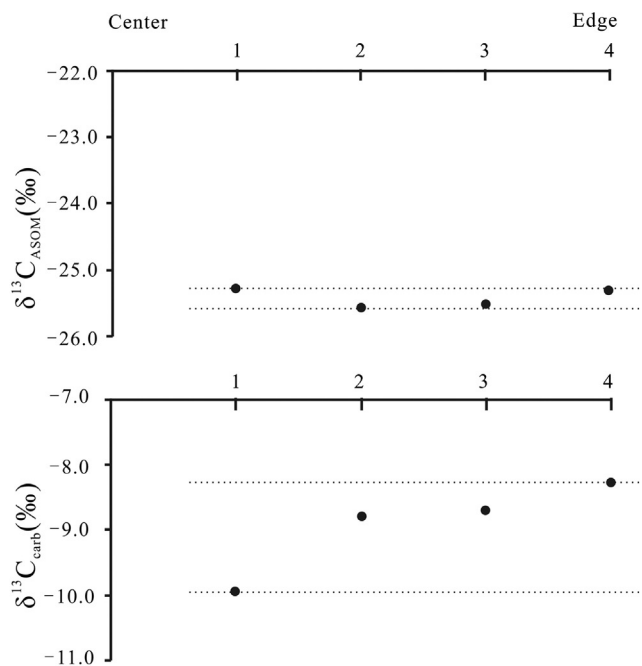
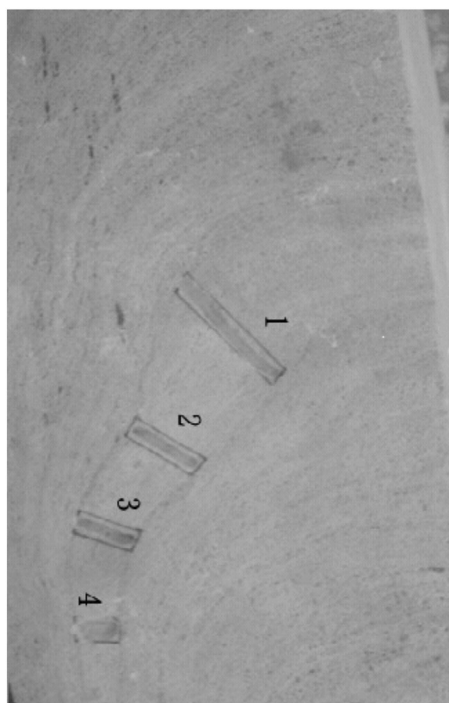


**Fig. 4.** (Left) The sampling sites along the growing band at 173 cm of HS-4. (Right) Variations of  $\delta^{13}\text{C}_{\text{ASOM}}$  and  $\delta^{13}\text{C}_{\text{carb}}$  values along the individual growing band. The average analytical error is about 0.2–0.4‰ for  $\delta^{13}\text{C}_{\text{ASOM}}$ , while the long-term repeatability for  $\delta^{13}\text{C}_{\text{carb}}$  is 0.1‰.

record shows relatively higher values during 9–8 ky BP and then varies around an average value of  $-11\text{‰}$  (Hu et al., 2008b), with a quite different trend than that of  $\delta^{13}\text{C}_{\text{ASOM}}$ .

The two surface soil samples (0–2 cm) show quite similar  $\delta^{13}\text{C}_{\text{ASOM}}$  results (soil-s:  $-23.7\text{‰}$  in July vs. soil-w:  $-24.2\text{‰}$  in November). The  $\delta^{13}\text{C}_{\text{ASOM}}$  values of the drip waters are  $-24.8\text{‰}$  in July (water-s) vs.  $-25.3\text{‰}$  in November (water-w) 2012, and are similar to the topmost sample of HS-4 stalagmite ( $-25.4\text{‰}$ ; ~12 yr BP).

## 4. Discussion

### 4.1. Origin of ASOM in HS-4 stalagmite

The similar FT-IR spectra of the overlying soil, drip waters and stalagmites clearly provide evidence that the ASOM preserved in HS-4 mainly originates from the overlying soil, with a quite limited contribution from cave bedrock. In addition, the FT-IR spectra of the overlying soils are comparable with those of FAs, suggesting that FAs are the dominant contributor of ASOM. Organic acids, mainly FAs and humic acids (HAs), make up about 60–70% of the total organic carbon in soils (Senesi, 1993; McGarry and Baker, 2000). FAs are soluble in water at any pH, whereas HAs are insoluble in water with  $\text{pH} < 2$  (Senesi, 1993). In fact, many studies demonstrate that fulvic-like matter is the dominant natural fluorescent substances in cave drip waters (Baker and Genty, 1999) and speleothems (e.g. Baker et al., 1998; McGarry and Baker, 2000; Blyth et al., 2008). However, we could not exclude the contribution of non-humic and fulvic-like substances to ASOM in this study, and we hence refer to it as ASOM rather than FA.

### 4.2. Climatic implications of stalagmite $\delta^{13}\text{C}_{\text{ASOM}}$

Because the  $\delta^{13}\text{C}_{\text{ASOM}}$  values in HS-4 stalagmite are independent of fractionation occurring during degassing and calcite deposition (Fig. 4), the majority of the  $\delta^{13}\text{C}_{\text{ASOM}}$  fluctuations must originate from the overlying vegetation and soil ecosystem. Fluorescence studies of speleothem organic acids also support that soil cover, vegetation and associated climate changes exert more important influence on this stalagmite organic matter proxy than internal cave processes (McGarry and Baker, 2000).

#### 4.2.1. Influence from vegetation

Heshang Cave (294 m above the sea level) forms in Cambrian dolomite and the overlying hillsides have an altitude up to 900 m (Hu et al., 2008a). According to the vegetation in the nearby Houhe National Nature Reserve ( $29^{\circ}59' - 30^{\circ}10' \text{N}$ ,  $110^{\circ}22' - 110^{\circ}52' \text{E}$ ) in the Wufeng Tujiazuo Minority Autonomous County of Hubei Province, the region between 400 and 1150 m is dominated by evergreen broadleaf (Li et al., 2005). In the study region,  $\text{C}_3$  plants dominate the vegetation, with a minor contribution from  $\text{C}_4$  plants (Cui et al., 2008). For  $\text{C}_3$  plants, environmental factors, especially temperature and humidity, can mediate the carbon isotope fractionation during photosynthesis (Farquhar et al., 1989; Ménot and Burns, 2001). Vascular plants can adjust their leaf stomata to adapt to humidity changes. An increase of humidity is usually accompanied by an increase of stomatal conductance and  $\delta^{13}\text{C}_{\text{leaf}}$  (Kohn, 2010). The influence of temperature on  $\text{C}_3$  plant  $\delta^{13}\text{C}$  is relatively complex. Temperature can directly control enzymatic activity in vegetation, affect metabolic capability and finally result in change of  $\delta^{13}\text{C}$ . In addition, temperature can affect other environmental factors and then influence the composition of carbon isotopes in vegetation.

#### 4.2.2. Influence from soil processes

Other than the influence from vegetation changes, microbial activity is another important factor to manifest  $\delta^{13}\text{C}_{\text{ASOM}}$  signals preserved in speleothems.

Dissolved organic matter (DOM) is the main form in which organic carbon is transported downward into the subsoil layers and finally

into the groundwater (Batiot et al., 2003; Ban et al., 2008). Soil DOM is generally divided into two groups, the hydrophobic (HPO) and hydrophilic (HPI) fractions (e.g. Aiken and Leenheer, 1993; Nakanishi et al., 2012). The HPO fraction consists mainly of aromatic lignin-derived compounds and has relatively longer fluorescence wavelength than the HPI fraction (Baker et al., 1998; McGarry and Baker, 2000). These hydrophobic materials are relatively stable against biodegradation (Kalbitz et al., 2003). The HPI fraction, in contrast, contains less aromatic structures but more carbohydrates, amino acids and hydroxyl groups. This fraction mainly derives from recent litter and photosynthates (Guggenberger et al., 1994). The HPI fraction is more labile relative to the HPO fraction (Qualls and Haines, 1992; Jandl and Sollins, 1997; Kalbitz et al., 2003). Corresponding with their consistent difference, the carbon isotopic signatures of HPI are commonly heavier than that of HPO (Kaiser et al., 2001, 2004; Kalbitz and Kaiser, 2008; Nakanishi et al., 2012).

If microbial activity can change the HPI/HPO ratio of soil DOM, this activity would finally mediate the carbon isotopic composition of ASOM preserved in stalagmites. Several factors can control microbial degradation on DOM. The first possible factor is the exposure time to microbial degradation. Under conditions with decreased effective precipitation, the residence time of organic matter in the soil and ground water will be extended, increasing the possibility of it being degraded before being preserved in stalagmites. If the exposure time in soil is the dominant process to control the signature of  $\delta^{13}\text{C}_{\text{ASOM}}$ , we would expect lighter values of  $\delta^{13}\text{C}_{\text{ASOM}}$  under drier conditions. In such conditions, due to the prolonged residence time, the HPI/HPO ratio will be smaller and the  $\delta^{13}\text{C}_{\text{ASOM}}$  will be lighter. Under such a scenario, the relatively negative  $\delta^{13}\text{C}_{\text{ASOM}}$  values from 9 to 4 ky BP may indicate that it was relatively dry in the study region. In contrast, the less negative  $\delta^{13}\text{C}_{\text{ASOM}}$  values from 4 to 0 ky BP suggest that it was relatively wet.

Temperature is another important factor to control microbial activity and associated degradation. The rates of microbial activity are normally higher in warmer conditions (Fang and Moncrieff, 2001; Dong et al., 2010). The study region is characterized by warm and humid climate. Consequently, under warmer humid conditions, microbes will preferentially degrade the HPI fraction, resulting in a relatively low HPI/HPO ratio and more negative  $\delta^{13}\text{C}_{\text{ASOM}}$ . The above deduction is supported by correlation analysis between the HS-4  $\delta^{13}\text{C}_{\text{ASOM}}$  record and the paleo-temperature record derived from the branched fatty alcohol ratio  $\text{BNA}_{15}$  recorded in the nearby Dajiuhu peatland (Huang et al., 2013) (Fig. 3). Interestingly, if we take consideration of the dating error and attribute horizons from the two sequences with age difference less than 50 yr as synchronous age, these two sequences correlate negatively ( $r = -0.48$ ,  $n = 57$ ,  $p < 0.001$ ; Fig. 5), with more negative  $\delta^{13}\text{C}_{\text{ASOM}}$  values appearing in warmer conditions. There are also some inconsistencies between the  $\delta^{13}\text{C}_{\text{ASOM}}$  and the  $\text{BNA}_{15}$  record. For example, the  $\text{BNA}_{15}$  shows a general decreasing trend from 3 ka onwards, while the increasing trend of the  $\delta^{13}\text{C}_{\text{ASOM}}$  is punctuated by an interval with lighter values at ca. 2 ka (Fig. 3).

Caves are often thought of as severely resource-limited settings due to the absence of light. However, recent research highlights that caves also contain high microbial abundance (e.g. Northup and Lavoie, 2001; Novakova, 2009; Cuezva et al., 2012). Thus it is reasonable to deduce that DOM will experience further processing within the cave, which could further decrease the HPI/HPO ratio and  $\delta^{13}\text{C}_{\text{ASOM}}$  values.

Other than microbial degradation, other soil processes can also affect soil DOM and finally exert controls on  $\delta^{13}\text{C}_{\text{ASOM}}$ . In soil horizons, soil organic matter and clay form complexes. Because HPO fractions have relatively high affinity onto the clay surfaces (Kalbitz et al., 2003; Nakanishi et al., 2012), such a clay-organic matter interaction can alter the HPI/HPO ratio and the associated  $\delta^{13}\text{C}_{\text{ASOM}}$  values of the DOM in soils. A recent study conducted by Grybos et al. (2009) highlights that large quantities of DOM are dissolved under elevated pH conditions. The acid-sensitivity of soil DOM has also been proposed as the main cause of widespread increases in concentrations of DOM in the surface

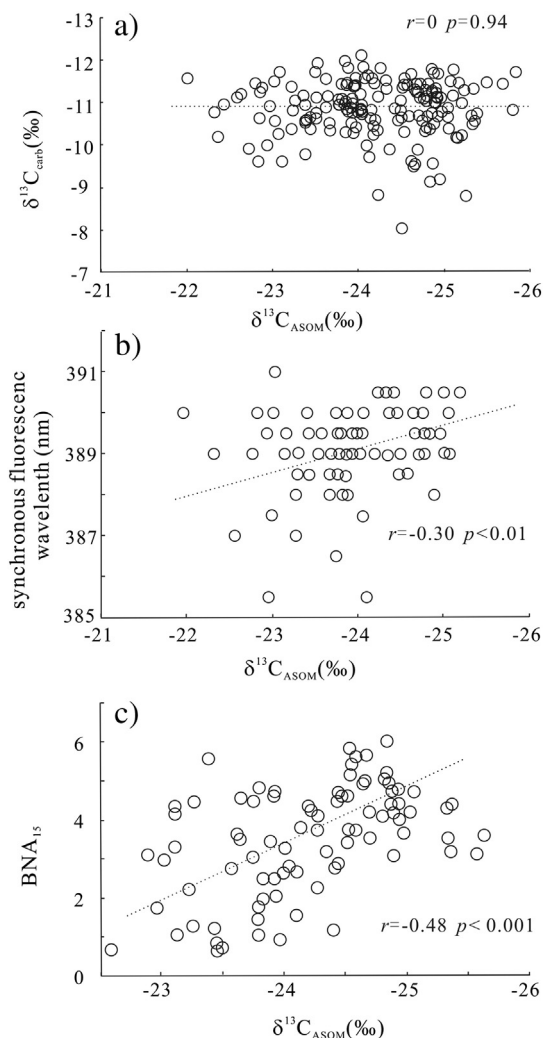


**Fig. 5.** Correlation analysis (a) between  $\delta^{13}\text{C}_{\text{ASOM}}$  and  $\delta^{13}\text{C}_{\text{carb}}$  (cited from Hu et al., 2008b); (b)  $\delta^{13}\text{C}_{\text{ASOM}}$  and the synchronous fluorescence wavelength; (c)  $\delta^{13}\text{C}_{\text{ASOM}}$  and BNA<sub>15</sub> ratio (cited from Huang et al., 2013). Because of the age difference, both  $\delta^{13}\text{C}_{\text{ASOM}}$  and BNA<sub>15</sub> records have been interpolated at 100-yr interval.

waters across North America and Northern and Central Europe (Monteith et al., 2007). In this case, the pH-derived dissolution process has the potential to mediate the  $\delta^{13}\text{C}_{\text{ASOM}}$  values in the overlying soils and underlying karst system.

In the monsoonal region of China, soil pH normally correlates with aridity, with relatively high pH values during dry conditions (Huang et al., 2008a; Yang et al., 2012). Soil profiles developed in karst regions normally contain high contents of cations, especially  $\text{Ca}^{2+}$  and  $\text{Mg}^{2+}$ , which can buffer the fluctuations of rainfall-derived pH shifts. However, in quite wet intervals or during heavy rain periods, the influence of rainfall can exceed the buffer capacity of soil cations and thus cause soil pH to decrease. Thus we still need to be cautious that, in relatively wet climates, pH in the soil profile overlying Heshang Cave will decrease and a greater proportion of HPO fraction will be absorbed onto clay surfaces. This process finally results in a relatively high HPI/HPO ratio and less negative  $\delta^{13}\text{C}_{\text{ASOM}}$  values in speleothem deposits.

In the above discussion, we use the HPI–HPO model to interpret how microbial activity affects the signature of  $\delta^{13}\text{C}_{\text{ASOM}}$ . Further research is necessary to support this model. Interestingly, because of the known relationship between dissolved organic matter fluorescence wavelength and hydrophobicity, we would expect to see a correlation between fluorescence wavelength and  $\delta^{13}\text{C}_{\text{ASOM}}$  if the HPI/HPO ratio is the dominant control on  $\delta^{13}\text{C}_{\text{ASOM}}$ . However, for the HS-4 stalagmite,  $\delta^{13}\text{C}_{\text{ASOM}}$  shows

a weak correlation with the synchronous fluorescence wavelength ( $r = -0.30$ ,  $p < 0.01$ ; Fig. 5). Such a relatively weak correlation suggests that factors other than the HPI/HPO ratio are also controlling stalagmite  $\delta^{13}\text{C}_{\text{ASOM}}$  in our stalagmite. It is therefore likely that microbial degradation of organic matter is just one competing process controlling the carbon isotope composition of the ASOM, along with the changes in vegetation structure and physiology, and physical factors affecting soil organic matter stability and transport.

## 5. Conclusions

This study presented first 9000-yr time series of EA-IRMS analysis of acid-solution organic matter isolated from the HS-4 stalagmite collected from Heshang Cave, central China. Spectroscopic analyses support that the ASOM mainly originates from the overlying soil. The  $\delta^{13}\text{C}_{\text{ASOM}}$  varies between  $-25.8\text{‰}$  and  $-22.0\text{‰}$ , with an average of  $-24.2\text{‰}$ . Comparisons between  $\delta^{13}\text{C}_{\text{ASOM}}$  and  $\delta^{13}\text{C}_{\text{carb}}$  in a single growth layer and the time series clearly show that  $\delta^{13}\text{C}_{\text{ASOM}}$  is not affected by kinetic fractionation during stalagmite formation. We hypothesize that the  $\delta^{13}\text{C}_{\text{ASOM}}$  record in HS-4 is controlled by both temperature and effective precipitation. The influence of temperature is mainly on the microbial degradation of soil organic matter, possibly with additional influences on the vegetation physiology. The availability of water can affect the length of time organic matter is exposed to microbial processing in soils. Under drier conditions, the exposure time of soil organic matter will be prolonged and lead to a higher degree of degradation, resulting in relatively low HPI/HPO ratios and more negative  $\delta^{13}\text{C}_{\text{ASOM}}$  values. Further evidence, such as from modern monitoring programs, would help test our hypothesis.

## Acknowledgments

This work was supported by 973 program (2011CB808800), the National Natural Science Foundation of China (Grants No. 41072262, 41371216, 41302145), and the China Postdoctoral Science Foundation (Grant No. 2013M531757). Miss Xiao Bai is thanked for her help during the organic carbon analysis. Jinxiang Zhang, Jiaoyang Ruan and Canfa Wang are acknowledged for their help during sample extraction and fieldwork. Prof. Philip A. Meyers is thanked for language editing. The two anonymous reviewers are acknowledged for their suggestions and comments that help us to improve the quality of this contribution.

## Appendix A. Supplementary data

Supplementary data to this article can be found online at <http://dx.doi.org/10.1016/j.chemgeo.2014.08.029>.

## References

- Aiken, G.R., Leenheer, J.A., 1993. Isolation and chemical characterization of dissolved and colloidal organic matter. *Chem. Ecol.* 8, 135–151.
- Baker, A., Genty, D., 1999. Fluorescence wavelength and intensity variations of cave waters. *J. Hydrol.* 217, 19–34.
- Baker, A., Genty, D., Smart, P.L., 1998. High resolution records of soil humification and palaeoclimate change from speleothem luminescence excitation-emission wavelength variations. *Geology* 26, 903–906.
- Baker, A., Wilson, R., Fairchild, I.J., Franke, J., Spötl, C., Matthey, D., Trouet, V., Fuller, L., 2011. High resolution  $\delta^{18}\text{O}$  and  $\delta^{13}\text{C}$  records climate from an annually laminated Scottish stalagmite and relationship with last millennium climate. *Glob. Planet. Chang.* 79, 303–311.
- Ban, F., Pan, G., Zhu, J., Cai, B., Tan, M., 2008. Temporal and spatial variations in the discharge and dissolved organic carbon of drip waters in Beijing Shihua Cave, China. *Hydrol. Process.* 22, 3749–3758.
- Batiot, C., Emblanch, C., Blavoux, B., 2003. Total Organic Carbon (TOC) and magnesium ( $\text{Mg}^{2+}$ ): two complementary tracers of residence time in karstic systems. *Compt. Rendus Geosci.* 335, 205–214.
- Blyth, A.J., Schouten, S., 2013. Calibrating the glycerol dialkyl glycerol tetraether signal in speleothems. *Geochim. Cosmochim. Acta* 109, 312–328.
- Blyth, A.J., Asrat, A., Baker, A., Gulliver, P., Leng, M.J., Genty, D., 2007. A new approach to detecting vegetation and land-use change using high resolution lipid biomarker records in stalagmites. *Quat. Res.* 68, 314–324.

- Blyth, A.J., Baker, A., Collins, M.J., Penkman, K.E.H., Gilmour, M.A., Moss, J.S., Genty, D., Drysdale, R.N., 2008. Molecular organic matter in speleothems and its potential as an environmental proxy. *Quat. Sci. Rev.* 27, 905–921.
- Blyth, A.J., Shutova, Y., Smith, C., 2013a.  $\delta^{13}\text{C}$  analysis of bulk organic matter in speleothems using liquid chromatography–isotope ratio mass spectrometry. *Org. Geochem.* 55, 22–25.
- Blyth, A.J., Smith, C.L., Drysdale, R.N., 2013b. A new perspective on the  $\delta^{13}\text{C}$  signal preserved in speleothems using LC–IRMS analysis of bulk organic matter and compound specific stable isotope analysis. *Quat. Sci. Rev.* 75, 143–149.
- Blyth, A.J., Jex, C.N., Baker, A., Khan, S.J., Schouten, S., 2014. Contrasting distributions of glycerol dialkyl glycerol tetraethers (GDGTs) in speleothems and associated soils. *Org. Geochem.* 69, 1–10.
- Cosford, J., Qing, H., Matthey, D., Eglinton, B., Zhang, M., 2009. Climatic and local effects on stalagmite  $\delta^{13}\text{C}$  values at Lianhua Cave, China. *Palaeogeogr. Palaeoclimatol. Palaeoecol.* 280, 235–244.
- Cuezva, S., Fernandez-Cortes, A., Porca, E., Pasic, L., Jurado, V., Hernandez-Marine, M., Serrano-Ortiz, P., Hermosin, B., Canaveras, J.C., Sanchez-Moral, S., Saiz-Jimenez, C., 2012. The biogeochemical role of Actinobacteria in Altamira Cave, Spain. *FEMS Microbiol. Ecol.* 81, 281–290.
- Cui, J., Huang, J., Xie, S., 2008. Characteristics of seasonal variations of leaf *n*-alkanes and *n*-alkenes in modern higher plants in Qingjiang, Hubei Province, China. *Chin. Sci. Bull.* 53, 2659–2664.
- Dong, H., Jiang, H., Yu, B., Liu, X.Q., 2010. Impacts of environmental change and human activity on microbial ecosystems on the Tibetan Plateau, NW China. *GSA Today* 20, 4–10.
- Dreybrodt, W., Scholz, D., 2011. Climatic dependence of stable carbon and oxygen isotope signals recorded in speleothems: from soil water to speleothem calcite. *Geochim. Cosmochim. Acta* 75, 734–752.
- Duan, W., Tan, M., Ma, Z., Cheng, H., 2014. The palaeoenvironmental significance of  $\delta^{13}\text{C}$  of stalagmite BW-1 from Beijing, China during Younger Dryas intervals inferred from the grey level profile. *Boreas* 43, 243–250.
- Fairchild, I.J., Baker, A., 2012. *Speleothem Science: From Process to Past Environment*. Wiley-Blackwell, (432 pp).
- Fairchild, I.J., Treble, P.C., 2009. Trace elements in speleothems as recorders of environmental change. *Quat. Sci. Rev.* 28, 449–468.
- Fang, C., Moncrieff, J.B., 2001. The dependence of soil  $\text{CO}_2$  efflux on temperature. *Soil Biol. Biochem.* 33, 155–165.
- Farquhar, G.D., Ehleringer, J.R., Hubick, K.T., 1989. Carbon isotope discrimination and photosynthesis. *Annu. Rev. Plant Physiol. Plant Mol. Biol.* 40, 503–537.
- Frappier, A., Sahagian, D., González, L.A., Carpenter, S.J., 2002. El Niño events recorded by stalagmite carbon isotopes. *Science* 298, 565.
- Frisia, S., Fairchild, I.J., Fohlmeister, J., Miorandi, R., Spötl, C., Borsato, A., 2011. Carbon mass-balance modelling and carbon isotope exchange processes in dynamic caves. *Geochim. Cosmochim. Acta* 75, 380–400.
- Genty, D., Baker, A., Massault, M., Proctor, C., Pons-Branchu, E., Hamelin, B., 2001. Dead carbon in stalagmites: carbonate bedrock paleodissolution vs. ageing of soil organic matter. Implications for  $^{13}\text{C}$  variations in speleothems. *Geochim. Cosmochim. Acta* 65, 3443–3457.
- Genty, D., Blamart, D., Ouahdi, R., Gilmour, M., Baker, A., Jouzel, J., Van-Exter, S., 2003. Precise dating of Dansgaard–Oeschger climate oscillations in western Europe from stalagmite data. *Nature* 421, 833–837.
- Grybos, M., Davanche, M., Gruau, G., Petitjean, P., Pédrot, M., 2009. Increasing pH drives organic matter solubilization from wetland soils under reducing conditions. *Geoderma* 154, 13–19.
- Guggenberger, G., Zech, W., Schulten, H.-R., 1994. Formation and mobilization pathways of dissolved organic matter: evidence from chemical structural studies of organic matter fractions in acid forest floor solutions. *Org. Geochem.* 21, 51–66.
- Hu, C., Henderson, G.M., Huang, J., Chen, Z., Johnson, K.R., 2008a. Report of a three-year monitoring programme at Heshang Cave, Central China. *Int. J. Speleol.* 37, 143–151.
- Hu, C., Henderson, G.M., Huang, J., Xie, S., Sun, Y., Johnson, K.R., 2008b. Quantification of Holocene Asian monsoon rainfall from spatially separated cave records. *Earth Planet. Sci. Lett.* 266, 221–232.
- Huang, D., Lee, X., Jiang, W., Zhao, Y., Ding, W., 2008a. Geographic variation of carbonate content and pH in surface soil in East Central Asia: significance as climate proxies. *Geochimica* 37 (2), 129–138 (in Chinese with English abstract).
- Huang, X., Cui, J., Pu, Y., Huang, J., Blyth, A.J., 2008b. Identifying “free” and “bound” lipid fractions in stalagmite samples: an example from Heshang Cave, Southern China. *Appl. Geochem.* 23, 2589–2595.
- Huang, X., Meyers, P.A., Jia, C., Zheng, M., Xue, J., Wang, X., Xie, S., 2013. Paleotemperature variability in central China during the last 13 ka recorded by a novel microbial lipid proxy in the Dajiuhe peat deposit. *The Holocene* 23, 1123–1129.
- Jandl, R., Sollins, P., 1997. Water-extractable soil carbon in relation to the belowground carbon cycle. *Biol. Fertil. Soils* 25, 196–201.
- Kaiser, K., Guggenberger, G., Zech, W., 2001. Isotopic fractionation of dissolved organic carbon in shallow forest soils as affected by sorption. *Eur. J. Soil Sci.* 52, 585–597.
- Kaiser, K., Guggenberger, G., Haumaier, L., 2004. Changes in dissolved lignin-derived phenols, neutral sugars, uronic acids, and amino sugars with depth in forested Haplic Arenosols and Rendzic Leptosols. *Biogeochemistry* 70, 135–151.
- Kalbitz, K., Kaiser, K., 2008. Contribution of dissolved organic matter to carbon storage in forest mineral soils. *J. Plant Nutr. Soil Sci.* 171, 52–60.
- Kalbitz, K., Schwesig, D., Schmerwitz, J., Kaiser, K., Haumaier, L., Glaser, B., Ellerbrock, R., Leinweber, P., 2003. Changes in properties of soil-derived dissolved organic matter induced by biodegradation. *Soil Biol. Biochem.* 35, 1129–1142.
- Kim, J.L., Bukau, G., Li, G.H., Duschner, H., Psarros, N., 1990. Characterization of humic and fulvic acids from Gorleben groundwater. *Fresenius J. Anal. Chem.* 338, 245–252.
- Kohn, M.J., 2010. Carbon isotope compositions of terrestrial C3 plants as indicators of (paleo)ecology and (paleo)climate. *Proc. Natl. Acad. Sci. U. S. A.* 107, 19691–19695.
- Li, Z., Wang, L., Huang, H., Tang, D., Pu, Y., Zheng, C., 2005. Situation and strategy of biodiversity conservation in the Houhe National Reserve, Hubei Province, China I. Situation and study of biodiversity. *J. Wuhan Bot. Res.* 23 (6), 592–600 (in Chinese with English abstract).
- Li, X., Hu, C., Liao, J., Bao, L., Mao, Q., 2014. An improved method for fluorescence analysis of dissolved organic matter in cave drip water. *Frontiers of Earth Science*. <http://dx.doi.org/10.1007/s11707-014-0439-6>, (in press).
- Lis, G.P., Mastalerz, M., Schimmelmann, A., Lewan, M.D., Stankiewicz, B.A., 2005. FTIR absorption indices for thermal maturity in comparison with vitrinite reflectance R0 in type-II kerogens from Devonian black shales. *Org. Geochem.* 36, 1533–1552.
- McDermott, F., 2004. Palaeo-climate reconstruction from stable isotope variations in speleothems: a review. *Quat. Sci. Rev.* 23, 901–918.
- McGarry, S.F., Baker, A., 2000. Organic acid fluorescence: applications to speleothem palaeoenvironmental reconstruction. *Quat. Sci. Rev.* 19, 1087–1101.
- Ménot, G., Burns, S., 2001. Carbon isotopes in ombrogenic peat bog plants as climatic indicators: calibration from an altitudinal transect in Switzerland. *Org. Geochem.* 32, 233–245.
- Monteith, D.T., Stoddard, J.L., Evans, C.D., de Wit, H., Forsius, M., Högåsen, T., Wilander, A., Skjelkvåle, B.L., Jeffries, D.S., Vuorenmaa, J., Keller, B., Kopáček, J., Vesely, J., 2007. Dissolved organic carbon trends resulting from changes in atmospheric deposition chemistry. *Nature* 450, 537–540.
- Nakanishi, T., Atarashi-Andoh, M., Koorashi, J., Saito-Kokubu, Y., Hirai, K., 2012. Carbon isotopes of water-extractable organic carbon in a depth profile of forest soil imply a dynamic relationship with soil carbon. *Eur. J. Soil Sci.* 63, 495–500.
- Northup, D.E., Lavoie, K.H., 2001. Geomicrobiology of caves: a review. *Geomicrobiol. J.* 18, 199–220.
- Novakova, A., 2009. Microscopic fungi isolated from the Domicia Cave system (Slovak Karst National Park, Slovakia). A review. *Int. J. Speleol.* 38, 71–82.
- Panno, S.V., Curry, B.B., Wang, H., Hackley, K.C., Liu, C.L., Lundstrom, C., Zhou, J., 2004. Climate change in southern Illinois, USA, based on the age and  $\delta^{13}\text{C}$  of organic matter in cave sediments. *Quat. Res.* 61, 301–313.
- Polk, J.S., van Beynen, P.E., Reeder, P.P., 2007. Late Holocene environmental reconstruction using cave sediments from Belize. *Quat. Res.* 68, 53–63.
- Polk, J.S., van Beynen, P., Asmerom, Y., Polyak, V.J., 2013. Reconstructing past climates using carbon isotopes from fulvic acids in cave sediments. *Chem. Geol.* 360–361, 1–9.
- Qualls, R.G., Haines, B.L., 1992. Biodegradability of dissolved organic matter in forest through fall, soil solution, and stream water. *Soil Sci. Soc. Am. J.* 56, 578–586.
- Rushdi, A.I., Clark, P.U., Mix, A.C., Ersek, V., Simoneit, B.R.T., Cheng, H., Edwards, R.L., 2011. Composition and sources of lipid compounds in speleothem calcite from southwestern Oregon and their paleoenvironmental implications. *Environ. Earth Sci.* 62, 1245–1261.
- Senesi, N., 1993. Organic substances in soil and water: natural constituents and their influences on contaminant behaviour. In: Beck, A.J., Jones, K.C., Hayes, M.B.H., Mingelgrin, U. (Eds.), *The Royal Society of Chemistry*, pp. 74–77 (Cambridge).
- Senesi, N., Miano, T.M., Provenzano, M.R., Brunetti, G., 1989. Spectroscopic and compositional comparative characterization of I.H.S.S. references and standard fulvic and humic acids of various origin. *Sci. Total Environ.* 81 (82), 143–156.
- Smailer, S.M., White, W., 2013. The luminescent humic substances in speleothems. *Appl. Geochem.* 36, 132–139.
- Stevenson, F.J., Goh, K.M., 1971. Infrared spectra of humic acids and related substances. *Geochim. Cosmochim. Acta* 35, 471–483.
- Turney, C.S.M., Bird, M.I., Roberts, R.G., 2001. Elemental  $\delta^{13}\text{C}$  at Allen’s Cave, Nullarbor Plain, Australia: assessing post-depositional disturbance and reconstructing past environments. *J. Quat. Sci.* 16, 779–784.
- van Beynen, P.E., Schwarcz, H.P., Ford, D.C., Timmins, G.T., 2002. Organic substances in cave drip waters: studies from Marengo Cave, Indiana. *Can. J. Earth Sci.* 39, 279–284.
- Xie, S., Yi, Y., Huang, J., Hu, C., Cai, Y., Collins, M., Baker, A., 2003. Lipid distribution in a subtropical southern China stalagmite as a record of soil ecosystem response to palaeoclimate change. *Quat. Res.* 60, 340–347.
- Yang, H., Ding, W., Zhang, C.L., Wu, X., Ma, X., He, G., Huang, J., Xie, S., 2011. Occurrence of tetraether lipids in stalagmites: implications for sources and GDGT-based proxies. *Org. Geochem.* 42, 108–115.
- Yang, H., Ding, W., Wang, J., Jin, C., He, G., Qin, Y., Xie, S., 2012. Soil pH impact on microbial tetraether lipids and terrestrial input index (BTI) in China. *Sci. China Earth Sci.* 55, 236–245.